VERIFICATION OF OPTICAL PAYLOAD CFRP STRUCTURE FOR SATELLITE THROUGH ANALYSIS AND SPACE QUALIFICATION TEST

Kyung-Joo Lee*, Hyun-Ung Oh*, Mun-Shin Jo, Dae-Jin Kim****
*** Image Information PEO, Agency for Defense Development, Yuseong P.O. Box 35, Daejeon, 305-600, Republic of Korea**
****Mechatronics Group, Samsung Tales, Republic of Korea**
* leekj94@msn.com, **ms77.jo@samsung.com

Abstract

This paper describes the development results of optical telescope CFRP structure with analysis and qualification test.

Structural analysis and space qualification tests were carried out with launch and in-orbit environments in order to verify the optical payload CFRP structure for satellite with optical, structural and dimensional stability point of view.

And structural stability is verified by coupon tests with statistical analysis for calculation Margin of Safety (MoS). Structural analysis with design load and modal analysis in order to prevent the dynamic coupling were performed. And thermo-elastic analysis with qualification temperature from on-orbit thermal analysis results was performed to verify the structural stability. After performed the analytical verification, space qualification tests with structural model(SM) were carried out with dynamic test (sin and random vibration test & sin burst (design load) test) and thermal cycle test for on-orbit structural stability. Optical performance (WFE: Wave front Error) with optics mounted on CFRP Bezel, structural stability with modal survey and 3-dimensional measurement with CMM were performed before and after the space qualification tests.

1 Introduction

Structure of space usage like satellite bus, payload telescope etc, was exposed by the launch environment from launcher system like acoustic, vibration, shock etc. And on orbit environment, structure should endure temperature change. Also structure should provide the dimensional stability for the optical performance in operation temperature range.

So high-modulus carbon fiber with Cyanate ester resin was chosen with Aluminum honeycomb core and invar. Stacking sequence design of using uni-directional lamina was performed for structure, thermal and optical requirements. After design the stacking sequence, laminate properties were verified with coupon test.

CFRP optical structure design was verified with analysis (modal, strength with design load, random vibration, distortion for optical performance and thermal elastic analysis) using coupon test results and qualification test (sin, random, shock and thermal cycle test).

2 Requirements

Main purpose of telescope structure is to provide the high dimensional stability interface in order to satisfy the optical design. Structure interface keeps the 3 mirrors, 4 lens and 1 on-board calibration unit. Lens for window is located on detector. Fig 1 shows the optical design layout.

These interface position should be stable through launch environment and under changing operation temperatures, temperature gradients, gravity release and the in-orbit moisture desorption.

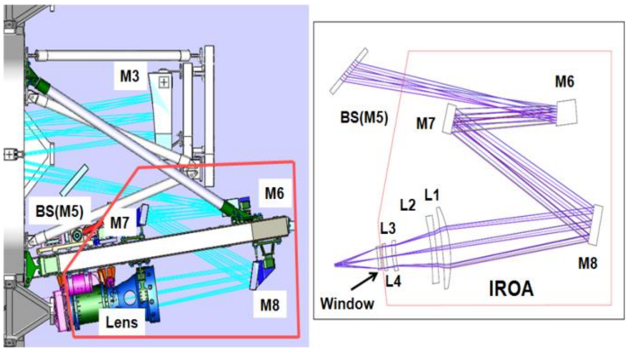

Fig. 1. Optical Design Layout

In order to design the optical telescope structure, requirements were considered with following items with launch and in-orbit condition.

Stiffness requirement is for avoiding the dynamic coupling with upper system and design load with quasi-static load is generally from MAC(Mass Acceleration Curve) at initial design phase. Temperature range for structure safety by thermal elastic analysis is from satellite level system orbit thermal analysis and is defined the survival temperature to qualification temperature

- *Mass : < 31.5kg*
- *Envelop : 880mm x 860mm x 760mm*
- *1st frequency(Stiffness) : > 120Hz*
- *Design Load : 25g*
- *Qual. Temperature range : -15~50^{o}C*

Optical requirements at in-orbit operation condition were defined with wave-front error (WFE) below 31.71nm$_{rms}$ from optical sensitivity analysis with following operation condition. Table 1 shows the in-orbit optical requirements with each environmental condition.

Table 1 In-orbit requirements

In-orbit Condition		Requirement
Uniform Temperature Change 12K		13.2 nm$_{rms}$
Temperature Gradients 1K	X	
	Y	
	Z	
Gravity Release	X	28.4 nm$_{rms}$
1g	Y	
	Z	
Moisture Desorption		5 nm$_{rms}$
Total		31.71 nm$_{rms}$

In launch condition, structure meets the vibration and shock environment. Vibration conditions are sinusoidal and random load. Shock load is from satellite separation mainly.

Table 2~4 show that sine, random vibration and shock environmental condition. These launch environments applied to the vibration analysis and qualification test.

Table 2 Sine vibration requirement

X, Y Axis (Lateral)		Z Axis (Axial)	
Frequency (Hz)	Qual. Accel. (g)	Frequency (Hz)	Qual. Accel. (g)
5 ~ 12	± 8mm	5~16	± 9.2mm
12 ~ 30	6.5 g	16~ 50	9.0 g
30 ~ 100	3.0 g	50 ~ 100	6.5 g

Table 3 Random vibration requirement

Frequency (Hz)	Qualification PSD (g^2/Hz)	Remarks
20	0.014	Duration Acceptance : 1 min Qualification: 2min All Axis(x,y,z)
70	0.05	
700	0.05	
2000	0.014	
Overall	8.2G$_{rms}$	

Table 4 Shock requirement

Frequency (Hz)	SRS (g)	Remark
100	8	
1515	270	
10000	270	
Qualification = 2 Actuations, Q=10		

2.2 Configuration Design

Figure 2 shows the configuration of CFRP optical telescope structure for verification with qualification level.

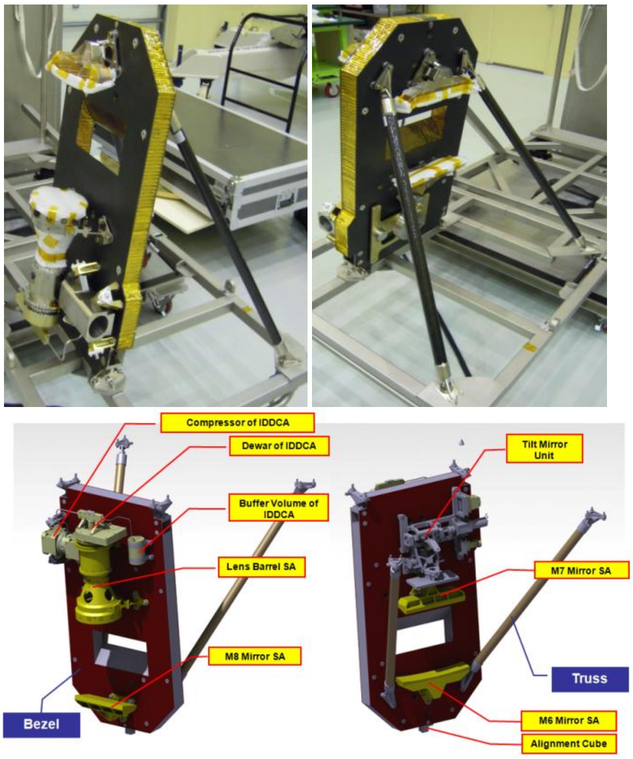

Fig. 2. Configuration of Structure

CFRP optical telescope structure was to be composed with 1 bezel and 2 trusses. Bezel was making up to CFRP facesheet and Al core for mounting optical components, detector and on-boards unit. In the bezel, high précised tolerance inserts were located to align the optical components based on optical sensitivity and tolerance analyses for assembly and alignment. Each inserts were met the Invar shims for the alignment.

Trusses were used to meet the eigen-frequency requirement to increase the stiffness of bezel. Truss was composed with CFRP and Invar fittings applied for athermalization design to prevent thermal stress.

Bezel and truss had a vent hole to prevent the debonding at vacuum condition.

2.3 Material Selection

Fiber was selected to Toray M55J Ultra-High Modulus fiber by trade-off study in order to satisfy the frequency requirement (Young's modulus for Stiffness) and optical requirement (dimensionally stable CTE (Coefficient of Thermal Expansion) at operation temperature).

Resin was selected the Cyanate ester with considered to minimize the moisture desorption deformation at space vacuum environment.

Aluminum honeycomb core was selected the porosity type to avoid the defect or delamination when changing pressure to vacuum. Core type is 3/16 in Al5056 with considered compressive and shear mechanical properties..

Aluminum insert was chosen to Al7075 T7351 to prevent the SCC(Stress Corrosion Cracking).

Invar for end fitting parts is Invar36 and Titanium was selected for thermal isolation.

Polymers like film adhesive FM73M for bonding between CFRP and Al core, adhesive EA9394 for CFRP to Invar fitting, and potting compound STYCASE 2651 for Al insert fixation were selected to consider the out-gassing requirement to TML(Total Mass Loss) $<$ 1% and CVCM(Collected Volatile Condensable Materials) $<$ 0.1%.

2.4 CFRP Stacking Angle Design

Stacking angle design was performed to be based on the selected CFRP uni-direction lamina ply properties using CLT (Classical Laminate Theory).

After calculating the laminate properties like young's modulus, shear modulus, CTE and CME using CLT with M55J and Cyanate ester resin, coupon test was done to verify the laminate properties.

Coupon test's results also were used to do the modal, structural stability and distortion analysis.

Figure 3 shows the coupon test location of structure. Except the CFRP tests (Tensile, Shear, CTE and density), bending, shear and flat wise tensile tests were performed to verify the structural bonding stability. These strength results were used to calculate the margin of safety(MoS) after statistical treatment of A-value.

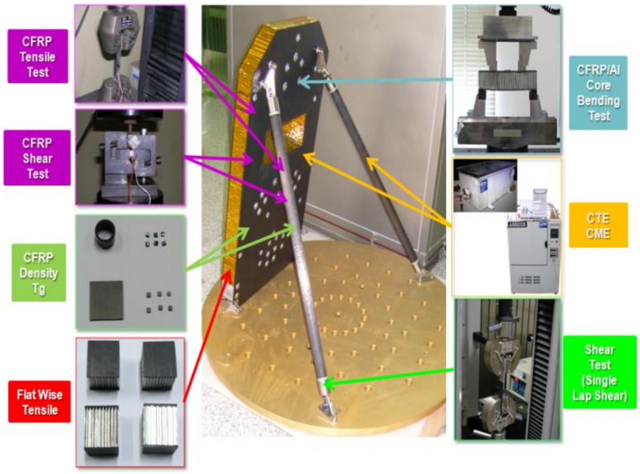

Fig. 3. Coupon test location

Table 5 and 6 show the laminate properties of facesheet on bezel and tube on truss. When calculating the maximum moisture strains with CME, TML was considered to 0.3%. When doing the TML and CVCM coupon test, TML was lower than 0.1%. So CME did not be tested.

Table 5 Laminate properties of facesheet in bezel.

Material Properties		Unit	CLT	Coupon Test Result
Young's Modulus	E_{11}	MPa	171400	173700
	E_{22}	MPa	38500	35700
Poisson's Ratio	ν_{12}	-	0.873	
Shear Modulus	G_{12}	MPa	43000	85977
	G_{23}	MPa	2600	61501
	G_{13}	MPa	3700	
CTE	α_1	1/K	$-1.33E^{-06}$	$-1.29E^{-06}$
	α_2	1/K	$2.26E^{-06}$	$2.89E^{-06}$
Density	ρ	Kg/cm³	1608	1600
Max. Moisture Strain *(CME)*	ε_1	-	$-2.188E^{-06}$ *($-6.564E^{-07}$)*	-
	ε_2	-	$2.312E^{-04}$ *($6.936E^{-05}$)*	-

Table 6 Laminate properties of tube in truss

Material Properties		Unit	CLT	Coupon Test Result
Young's Modulus	E_{11}	MPa	157600	152856
	E_{22}	MPa	64100	60400
Poisson's Ratio	ν_{12}	-	0.554	
Shear Modulus	G_{12}	Mpa	43100	49159
	G_{23}	MPa	2800	51986
	G_{13}	MPa	3500	
CTE	α_1	1/K	$-9.612E^{-07}$	$-1.17E^{-06}$
	α_2	1/K	$6.96E^{-07}$	$1.71E^{-06}$
Density	ρ	Kg/cm³	1608	1600
Max. Moisture Strain *(CME)*	ε_1	-	$2.2E^{-05}$ *($6.6E^{-06}$)*	-
	ε_2	-	$1.294E^{-04}$ *($3.882E^{-05}$)*	-

2.5 Analysis

In order to verify the requirement using analysis, analyses were performed to following contents.

- *Structure Analysis*
  - *Modal Analysis*
  - *Quasi-static load Analysis*
  - *Thermal Elastic Analysis*
- *Vibration Analysis*
- *Distortion Analysis*
  - *1K uniform temperature change*
  - *1K gradient temperature change*
  - *1g gravity release*
  - *Moisture release*

2.5.1 Finite Element Model(FEM)

In order to verify the requirement using analysis, FEM was built like Figure 3.

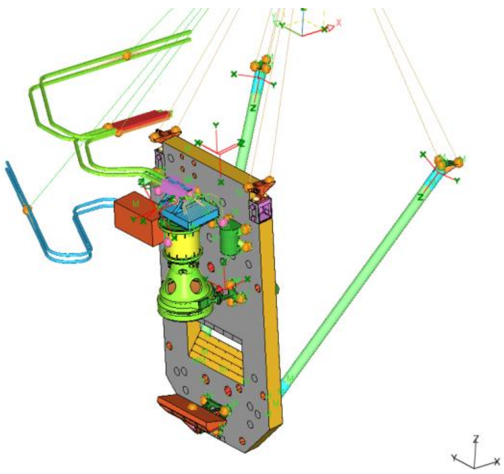

Fig. 4. Finite Element Model

At initial phase of design, FEM was composed with rumpled mass of mounting components. After done critical design, very fine mesh was used to analyze the optical component's surface error at nano-meter unit level.

2.5.2 Modal Analysis

In order to verify the stiffness requirement over 120Hz, modal analysis was performed.

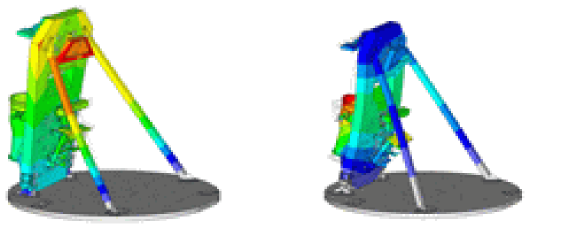

(a) 1st Mode (Rotation) (b) 2nd Mode (Bending)

Fig. 5. Modal analysis results

1st frequency is 137.8Hz with torsion mode and 2nd frequency is 148.9 Hz with bending mode. Figure 4 shows the modal analysis results.

2.5.3 Strength Analysis

Quasi-static load (Design load) and thermal elastic analyses were performed to verify the structural stability. Requirement is MoS>0. In equation 1, allowable stresses were used from coupon test results. Applied safety factor (SF) is like following.

$$MoS = \frac{Allowable\ Stress}{Applied\ Stress\ \times SF} - 1 \qquad (1)$$

Applied Safety Factor (SF):

- Metallic Materials Yield = 1.25
- Metallic Materials Ultimate = 1.4
- CFRP Ultimate = 2.0
- Adhesive Bonded Junction = 2.0
- Inserts and Joints Yield =1.5
- Inserts and Joints Ultimate = 2.0
- Joints gapping and slipping =1.15

Figure 6 shows the summary of MoS at design load 25g.

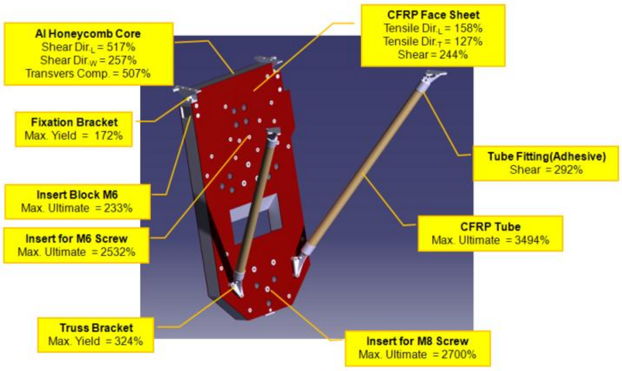

Fig. 6. MoS summary by design load 25g

Figure 7 shows the summary of MoS of joint screws by design load. And figure 8 shows the MoS of inserts bonding parts.

Figure 9 shows the -15°C thermal elastic results summary. And figure 10 shows the 50°C results summary. Thermal elastic reference temperature is 20°C because 20°C is the assembly, integration and alignment temperature.

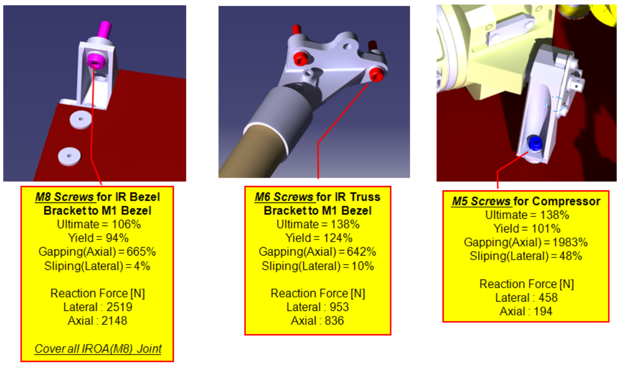

Fig. 7. MoS summary of joint screws by design load 25g

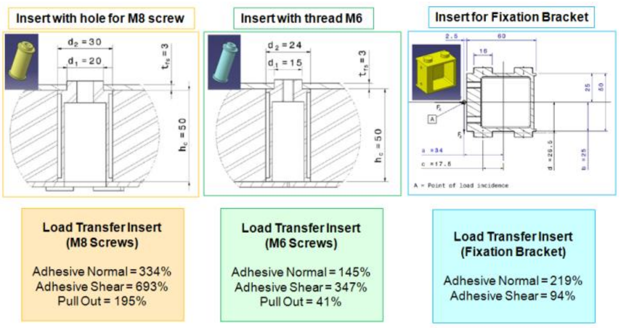

Fig. 8. MoS of inserts bonding parts by design load 25g

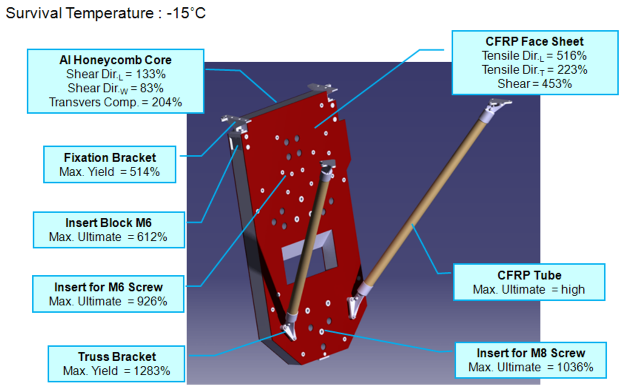

Fig. 9. MoS summary of thermo-elastic analysis of -15°C

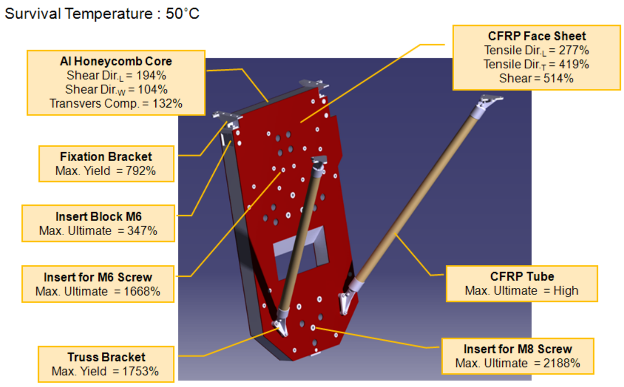

Fig. 10. MoS summary of thermo-elastic analysis of -50°C

For the structural stability point of view, structure can be endured at launch and in-orbit thermal condition with analytic method.

2.5.4 Vibration Analysis

In early design phase, conservative design load from MAC was used for checking the structural safety. After finished the detail design, structural stability should be checked by dynamic analysis because dynamic load may be greater than static design load and cause the coupling with each components.

And the other object of vibration analysis is the prediction of notching profile to prevent over-test at vibration test.

Because CFRP Structure stiffness requirement and modal analysis results gave the over 100Hz, random vibration analysis was performed except sine vibration at lower frequency excitation.

Random input PSD was come from qualification level in table 3 and is put to the mounting interface position.

Figure 11 shows the analysis results and Table 7 is the comparison the 3-sigma reaction force with overall g_{rms} from vibration analysis and the reaction force from quasi-static load 25g.

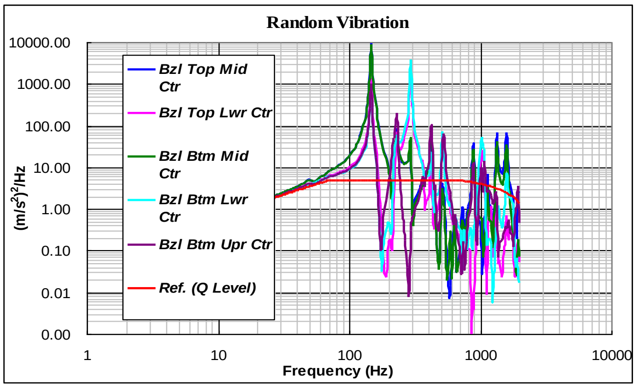

Fig. 11. Random vibration analysis results

Table 7 Comparison quasi-static analysis with random vibration analysis

Components	Max. I/F Force from Quasi-Static Load (N)			Reaction Force from Random Analysis (N)			Ratio (Quasi-Static I/F Force / Random Analysis I/F Force)
	X	Y	Z	X	Y	Z	Req. > 1
M6 SA	746.4	795.2	1262.4	465.7	666.3	626.7	1.89
M7 SA	518.7	1376.2	1568.7	752.6	497.7	586.0	2.08
M8 SA	543.6	1517.4	1717.8	799.0	872.6	774.7	1.97
Lens SA	1900.4	1099.4	1406.3	1570.1	1095.8	1720.0	1.10
TMU	1441.5	1009.0	314.0	615.1	524.6	765.9	1.88

In table 7, interface force of quasi-static loads are greater than random vibration interface force with overall g_{rms} multiple 3sigma value

Thus structural safety was guaranteed because MoS of quasi-static load analysis was positive.

2.5.5 Distortion Analysis

Distortion analysis is for the optical performance at in-orbit condition like following environment. Space condition with operating temperature condition with 1g gravity and moisture release should be considered for optical performance.

- 1K uniform temperature change
- 1K gradient temperature change
- 1g gravity release
- Moisture release

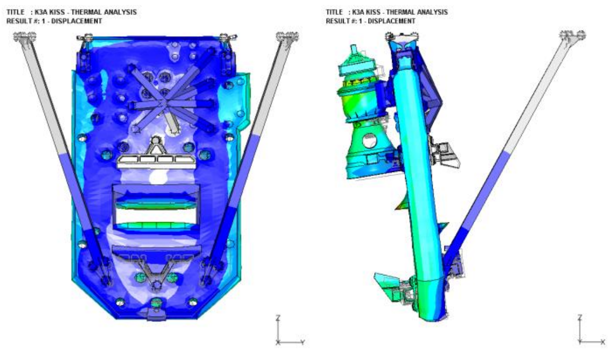

Fig. 12. Example of distortion analysis with 12K uniform temperature change

Figure 12 is the analysis results of uniform temperature change and other conditions also were performed. Table 8 shows that summary of distortion analysis. WFE requirements were come from optical sensitivity analysis and budgeting.

Table 8 Distortion analysis results

List of Distortion Analysis		WFE Req. (nm_{rms})	WFE (nm_{rms})		
			All condition	Assembly Condition (Only y-direction gravity)	Each Condition (RMS)
Temperature Change 12K		13.2	9.6216	9.6216	9.6216
Tempera-ture Gradient 1K	X		0.3188	0.3188	0.5833
	Y		0.1249	0.1249	
	Z		0.4723	0.4723	
Gravity Load 1g	X	28.4	5.9710	-	12.6632
	Y		7.8512	7.8512	
	Z		7.9413	-	
Moisture Desorption		5	2.3985	2.3985	2.3985
Total		31.71	16.094	12.661	N/A

Gradient and uniformity of temperature were from in-orbit thermal analysis and these temperature conditions have a margin for worst case. Gravity load was considered Y-axis only, because Y-axis is the assembly and integration axis. Moisture desorption is the reason to use the CFRP.

So total distortion WFE requirement with RMS values was worst case value and all analysis cases were fulfill with the requirements.

2.6 Qualification Test

After verify with analysis, qualification test was performed with using structure model(SM) according to AIT flow.

Test items are sine/random vibration and shock for launch environment and thermal cycle for in-orbit environment. Test level is shown in paragraph 2 requirements.

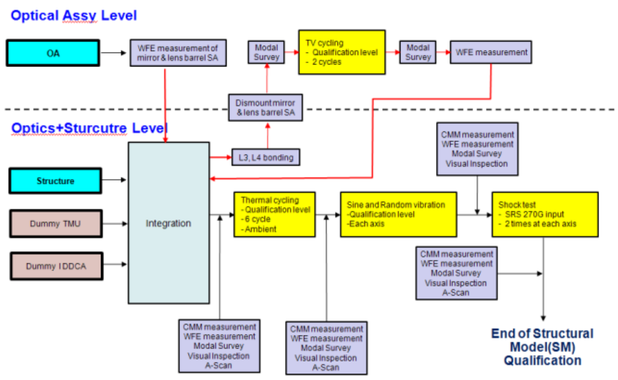

Fig. 13 Qualification Test Flow with SM

Test tolerances were referred to ECSS-E-10-03A Testing.

In order to check the structural safety and optical performance before and after each tests, visual inspection, modal survey, 3D measurement of dimension, WFE measurement for optical surface and ultrasonic inspection of bonding layer were performed. Inspection items' requirements are like following before and after test.

- Modal Survey(Freq. Change) : < 5% difference
- WFE change : < 25nm_{rms}
- 3D measurement : < 0.1mm
- Visual and NDT inspection : No damage

Vibration Test configuration is figure 14.

Fig. 14. Vibration test configuration (ex. X-axis)

2.6.1 Sine Burst Test

In order to verify the design load 25g, sine burst test was performed below 1/3 of natural frequency for static load condition.

After test, there was no structural characteristic change. Figure 15 shows the sine burst test profile and CG response of structure.

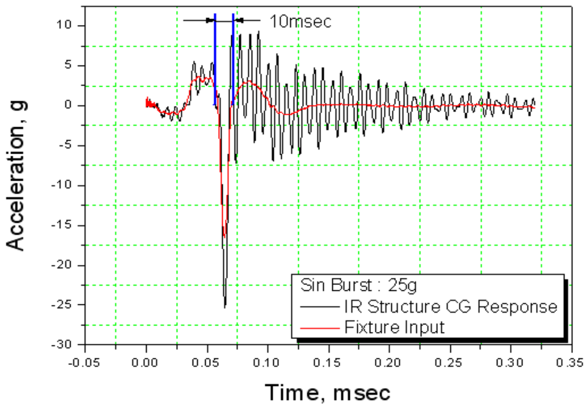

Fig. 15. Sine burst test profile and response

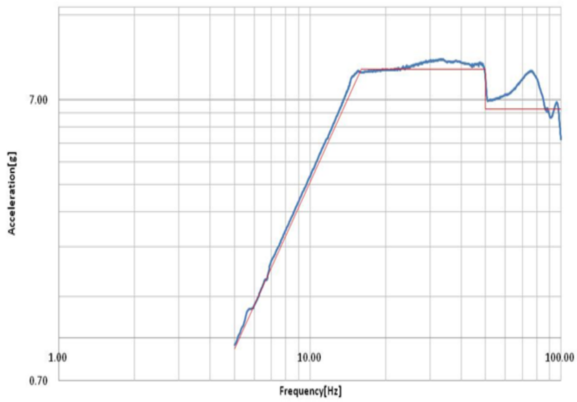

Fig. 16. Sine vibration test profile and CG response (ex. Z-axis)

2.6.2 Sine Vibration Test

Low frequency accelerating condition of structure was confirmed with sine vibration test. And maximum axis is Z-axis of LOS direction.

Figure 16 shows the test profile and response of CG point on maximum Z-axis.

Sine vibration test was performed x, y, z axis

2.6.3 Random Vibration Test

Random vibration test was done with notched profile of initial flat PSD profile to prevent the over specified test. Notching profile was estimated with from random vibration analysis response and low level modal survey result. Figure 17 shows the random vibration notching test profile example vs. flat PSD vs. controlled input specification of x-axis test. Y and Z-axes test profiles are different from each other axis because all axes dynamic responses are different. Notching level was controlled with based on each components design load

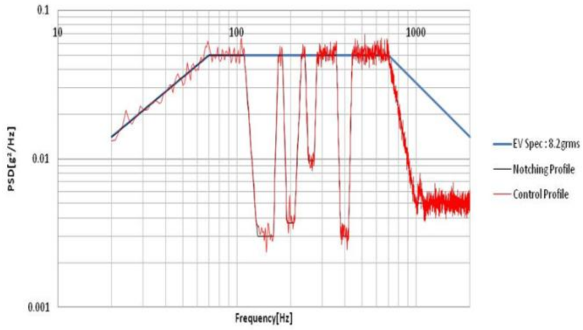

Fig. 17. Random vibration test profile of X-axis (Specification vs. Notching Ref. vs. Controlled)

Figure 18 shows the response of CG point with notching profile. Input PSD was controlled by design load 25g.

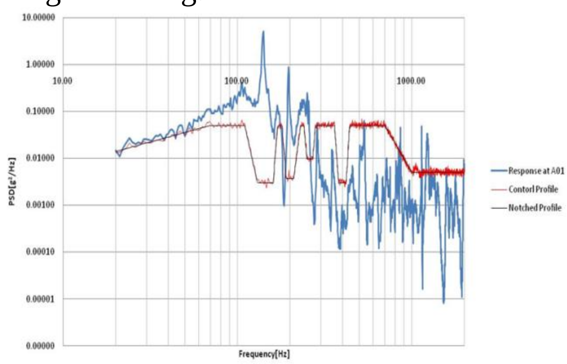

Fig. 18. Random vibration Response on CG

2.6.4 Shock Test

For the shock environmental qualification test, 2 actuations were done with 270g SRS. Figure 19 shows the controlled input SRS and CG response with test tolerance ±6dB.

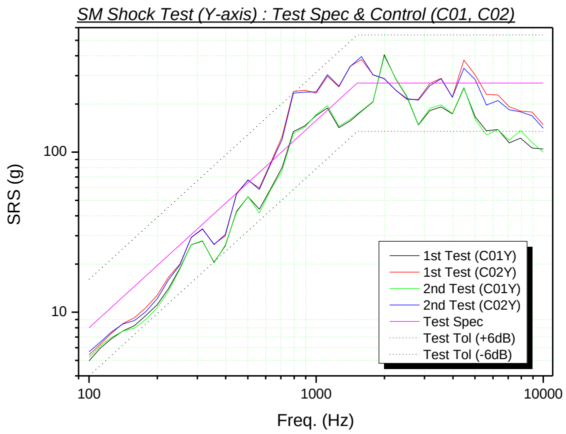

Fig. 19. Shock test profile and CG response.

2.6.5 Thermal Cycle Test

Thermal cycle test was performed to verify the thermal stress at in-orbit condition. Thermal cycle test was chosen rather than thermal vacuum test because there are no vacuum sensitivity parts in structure parts.

Mounting MGSE of structure was simulated for CFRP with flexure design in order to prepare abnormal thermal deformation. Figure 20 shows the test configuration and figure 21 shows the thermal cycle test profile.

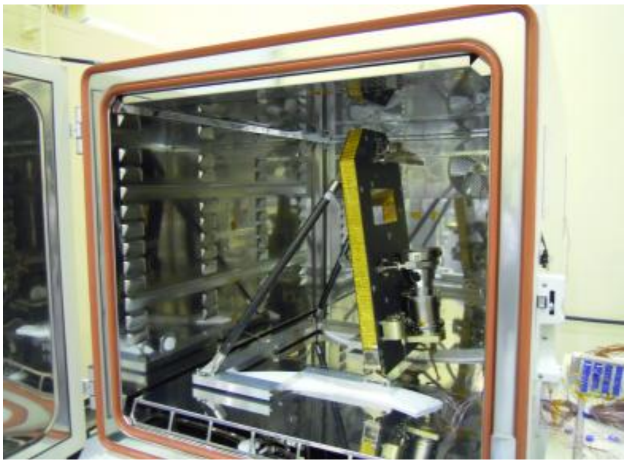

Fig. 20 Thermal cycle test configuration in TCT chamber with MGSE

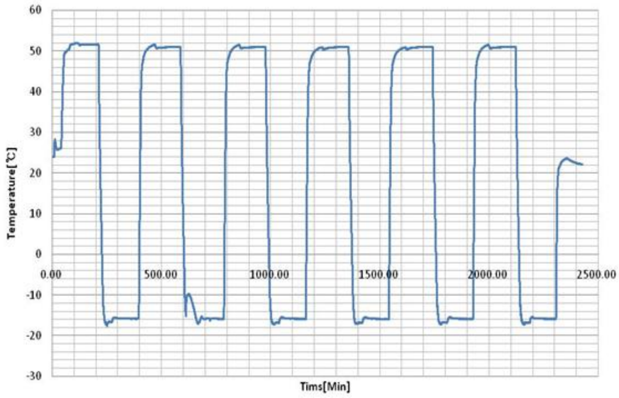

Fig. 21 Thermal cycle test profile

2.6.6 Inspection of tests

The visual inspection, 3D-dimensional measurement, modal survey for structural stability, WFE measurement of optical surface and NDT with ultrasonic inspection for bonding area of main load path part, were performed to inspect the structure before and after vibration, shock and thermal cycle tests.

The test results summary have been;

- Frequency difference of all tests was less than 5% with modal survey.
- WFE for optical surface performance change was less than 25nm$_{rms}$ with interferometer.
- Dimension with 3D measurement was less 0.1mm considered the test tolerance and condition.
- No damage and deformation have been detected with NDT ultrasonic and visual inspection.

Figure 22~24 show the 3D dimensional measurement, WFE measurement results and ultrasonic inspection configuration.

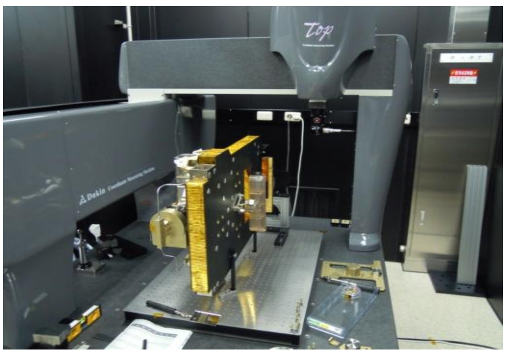

Fig. 22. 3D dimension measurement

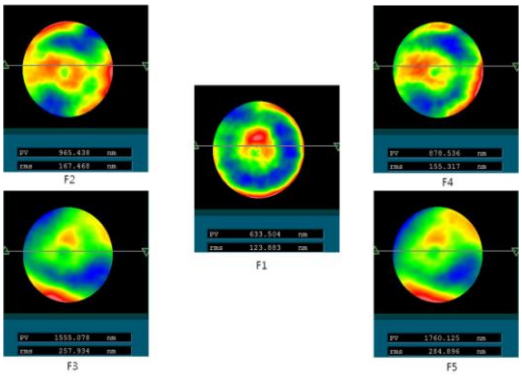

(a) before TCT

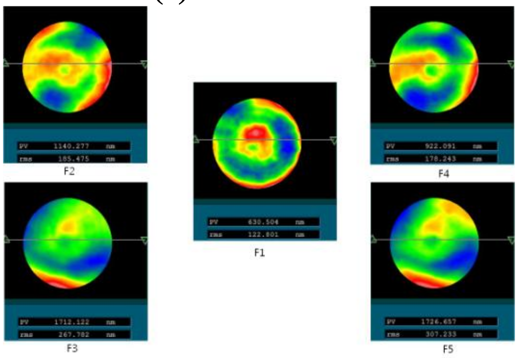

(b) before TCT

Fig. 23 WFE measurement for optical performance inspection

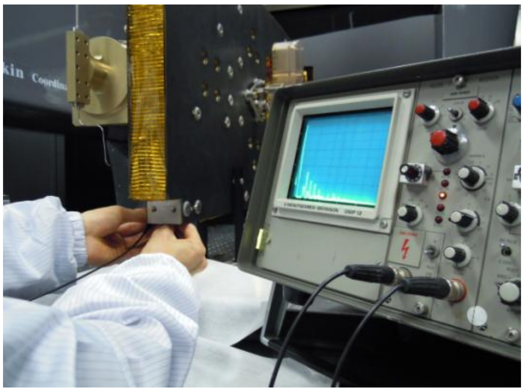

Fig. 24. Ultrasonic Inspection of bonding layer

3 Conclusion

Highly stable structure for the optical payload of satellite was developed out of CFRP material.

Designed CFRP structure has been fully verified with coupon test, analysis and qualification level test with launch and in-orbit environmental conditions.

These results will be applied to the next level system development for the space optical structure.

References

[1] J. Wijker, Spacecraft Structure, Springer, 2008.

[2] J. Wijker, Random Vibrations in Spacecraft Structures Design, Springer, 2009

[3] Department of Defense, Composite Materials Handbook, Vol. 1 Polymer Matrix Composites Guidelines for Characterization of Structural Materials, MIL-HDBK-17-1F, 2002.

[4] European Space Agency, Structural Materials Handbook Volume 1 Polymer Composites, ESA PSS-03-203, 1994

[5] European Space Agency, Structural Materials Handbook Volume 2 New Advanced Materials, ESA PSS-03-203, 1994.

[6] European Space Agency, Data for Selection of Space Materials, ESA PSS-01-701, 1994.

[7] European Space Agency, 1995, Adhesive Bonding Handbook for Advanced Structural Materials, ESA PSS-03-210

[8] European Space Agency, Threaded fasteners handbook, ECSS-E-HB-32-23A, 2010.

[9] Vinvent L. Pisacane & Robert C. Moore, Fundamentals of Space Systems, Johns Hopkins University, 1994.

[10] Wiley J. Larson & James R. Wertz, Space Mission Analysis and Design 2nd Edition, W.j. Larson and Microcosm, Inc. P430~468, 1995.

[11] European Space Agency, Insert Design Handbook, ECSS-E-HB-32-22A, 2011.

[12] Marc Trubert, Mass Acceleration Curve for Spacecraft Structure Design, Jet Propulsion Laboratory, 1989.

[13] MSC/Nastran, Nastran User's Manual, Ther Macneal-Schwendler Corporation

[14] NASA, Materials Selection List for Space Hardware Systems, MSFC-HDBK-527, 1988.

[15] European Space Agency, Space Engineering: Testing, ECSS-E-10-03A, 2002.

[16] European Space Agency, Space Engineering: Modal Surevey Assessment, ECSS-E-ST-32-11C, 2008.

[17] Department of Defense, Environmental Engineering Considerations and Laboratory Tests, MIL-STD-810F, 2000.

Copyright Statement